

ACKNOWLEDGMENT

This work was supported by SDIO/IST through ONR Contract #N00014-92-J-1993, NSF #DMR-8913524, Rochester Gas and Electric, and New York State Energy Research and Development Authority.

REFERENCES

1. D. Gupta, W. R. Donaldson, K. Kortkamp, and A. M. Kadin, in *Optically Activated Switching II* (SPIE, Bellingham, WA, 1992), Vol. 1632, p. 190.
2. S. K. Dhali and M. Mohsin, *Rev. Sci. Instrum.* **63**, 220 (1992).
3. T. Burke, J. Carter, M. Weiner, and N. Winsor, "Analysis of Current Multiplication Circuit Utilizing Programmed Inductive Elements (PIE)" (private communication); also presented at the IEEE's High Voltage Workshop, Monterey, CA, March 1988.
4. P. H. Ballentine, J. P. Allen, A. M. Kadin, and D. S. Mallory, *J. Vac. Sci. Technol. A* **9**, 1118 (1991).
5. J. H. Claasen, M. E. Reeves, and R. J. Soulen, Jr., *Rev. Sci. Instrum.* **62**, 996 (1991).
6. D. Gupta, W. R. Donaldson, K. Kortkamp, and A. M. Kadin, "Optically Triggered Switching of Optically Thick YBCO Films," presented at the 1992 Applied Superconductivity Conference, Chicago, IL, 23–28 August 1992, and to be published in *IEEE Transactions on Applied Superconductivity*.

2.D Strong K_{α} Emission in Picosecond Laser-Plasma Interactions

Since the development of ultrashort (≤ 1 -ps), high-peak-power laser systems, it has been possible to produce plasma with the picosecond duration of x-ray emission.^{1,2} A picosecond x-ray source may provide a useful probe of time-resolved phenomena with high temporal resolution. In ultrashort laser-plasma interactions, the relatively low x-ray conversion efficiency has been of particular concern. An increase of the conversion efficiency has been reported for the case of the laser pulse interacting with a preformed plasma, which has been created either by a small prepulse^{3,4} or a substantial level of amplified spontaneous emission (ASE).⁵ However, streak-camera measurements have shown that for a preformed plasma the x-ray pulse duration is much longer than in the case of a high-intensity-contrast laser pulse, i.e., no preformed plasma.^{1,6} A plasma produced by a p-polarized, high-intensity-contrast laser pulse is a promising candidate for an ultrashort x-ray source with high efficiency since it absorbs as much as 60% to 70% of the incident laser light.^{2,7} Measurements of the fast-ion blowoff indicated that a high fraction of the laser energy was carried by fast electrons.⁸ Hot electrons penetrating the target may induce K_{α} emission. Recently, K_{α} emission induced by hot electrons has indeed been observed in ultrashort laser-plasma interactions.^{9,10}

In this article details of K_{α} emission observed in the interaction of a picosecond, high-intensity-contrast, p-polarized laser pulse with a Si substrate coated with 0.2 μm to 2.5 μm Al are reported. Hot electrons are found to be the dominant source for K_{α} emission. The x-ray-source characteristics were inferred from high-resolution x-ray spectra, measurements of duration of emission, and source size. The analysis suggests that the K_{α} emission may have the potential to generate shorter x-ray pulses than, for example, resonance line emission since its temporal evolution depends on mechanisms like hot-electron generation rather than on recombination and cooling processes in the plasma.

Experimental Conditions

A chirped-pulse amplification and compression (CPAC) laser system¹¹ was used to generate 13-mJ, 1.3-ps, 1.05- μm pulses. Recent improvements in the laser design,¹² including the installation of a saturable dye cell (Kodak 2595 dye) after the compression gratings, have increased the intensity contrast from 10^3 to 5×10^5 . The duration of the prepulse is around 100 ps. The p-polarized laser light was focused onto the target at an angle of 60° . Because of the oblique incidence, the focal spot of the laser is elliptical with an area of $12 \mu\text{m} \times 24 \mu\text{m}$ (1/e intensity), leading to an irradiance of $4 \times 10^{15} \text{ W/cm}^2$ with a prepulse fluence of 0.8 J/cm^2 . The target material consisted of polished Si bulk material coated with 0.2 μm to 2.5 μm Al. The x-ray yield was measured with x-ray positive-intrinsic-negative (PIN) diodes filtered with 6 μm Al or 250 μm Be. The PIN diodes filtered with Al are sensitive to photon energies in the range of 0.9 keV to 1.56 keV and 2.5 keV to 15 keV, the PIN diodes filtered with Be to photon energies in the range of 2.5 keV to 15 keV. The PIN diodes were mounted at 0° to 20° with respect to the target normal. It was crucial to shield the PIN diodes with magnetic fields; otherwise, hot electrons would contribute substantially to the PIN-diode signal. The x-ray spectra were recorded with a von Hamos crystal spectrograph,¹³ which used a cylindrical pentaerythritol (PET) crystal with a 2-in. radius of curvature. The spectrograph collected the x-ray emission of the plasma at an angle of 40° with respect to the target normal. The calibration of the PET crystal and the Kodak double exposure film (DEF) was taken from published data.^{14,15} The signal of the PIN diodes agreed within 20% with the calibration of the spectrograph, provided that (consistent with an aged crystal) a Bragg reflection integral close to the Darwin zero extinction limit¹⁴ was assumed. About 30 shots were accumulated to obtain a single spectrum.

The duration of the x-ray emission was measured with an x-ray streak camera, which had a cathode made of a 2000- \AA parylene layer coated with 500 \AA Au and 1200 \AA CsI. X-ray filters, i.e., 1.5 μm Mylar, 6 μm Al, and 25 μm Be, were mounted in front of the streak-camera slit to get three channels with different spectral sensitivity. The Mylar channel detected soft x rays with photon energies exceeding 0.1 keV, the Be channel harder x rays above 1 keV, and the Al channel x rays from 0.9 keV to 1.56 keV and above 2.5 keV, respectively. Since no experimental value for the temporal resolution is currently available and an accurate calculation of the streak-camera response to short x-ray pulses is beyond the scope of this work, a somewhat simplified model, which assumes that the various broadening mechanisms are independent of each other and that the pulse shapes and secondary electron-energy distributions are Gaussian,¹⁶ was adapted. The finite slit width and the secondary-electron energy distribution of

CsI^{17} are predicted to limit the temporal resolution of the streak camera to ~ 7 ps. Space charge effects, especially for high current densities at the cathode, will further increase this value. Better resolution would require a higher extraction field, a higher sweep speed, and a cathode material with a smaller secondary-electron energy distribution, for example, KBr .¹

The source size of the x-ray emission was obtained from x-ray shadowgraphy, using a knife-edge technique.¹⁸ A razor blade was placed between the plasma and a DEF film filtered with $25 \mu\text{m}$ Be. The film was uniformly exposed, except for the region where the x-ray source was partially or completely covered by the razor blade. The derivative of the intensity distribution yielded the spatial-intensity profile of the x-ray source. An advantage of this setup is that for a fairly good signal-to-noise ratio a high spatial resolution can be achieved. In the experiment, the resolution was around $2 \mu\text{m}$ and was mostly limited by the smoothing of the raw data, which was performed in the numerical analysis of the x-ray shadowgraph.

Results and Discussion

1. X-Ray Yield

In the case of an Si target coated with $0.2 \mu\text{m}$ Al and a high-intensity-contrast laser pulse, i.e., a prepulse irradiance below 10^{10} W/cm^2 , resonance line emission (He_α), as well as strong K_α emission from both target materials, is present (Fig. 54.13). The Al K_α line from low ionization states of Al ($\text{Al}^{1+} - \text{Al}^{4+}$) is at 8.34 \AA , and the “shifted” Al K_α lines from $\text{Al}^{5+} - \text{Al}^{10+}$ are seen between 7.85 \AA and 8.32 \AA . The He_α line from He-like Al (Al^{11+}) is at 7.76 \AA . In the range 6.64 \AA to 7.13 \AA , similar to Al lines, are the Si K_α lines (shifted and unshifted) and the Si He_α line. The Al He_α line is emitted from the hot plasma ($k_B T_e \sim 300 \text{ eV}$) on the target surface. The Si and Al K_α emissions originate from colder material inside the target.

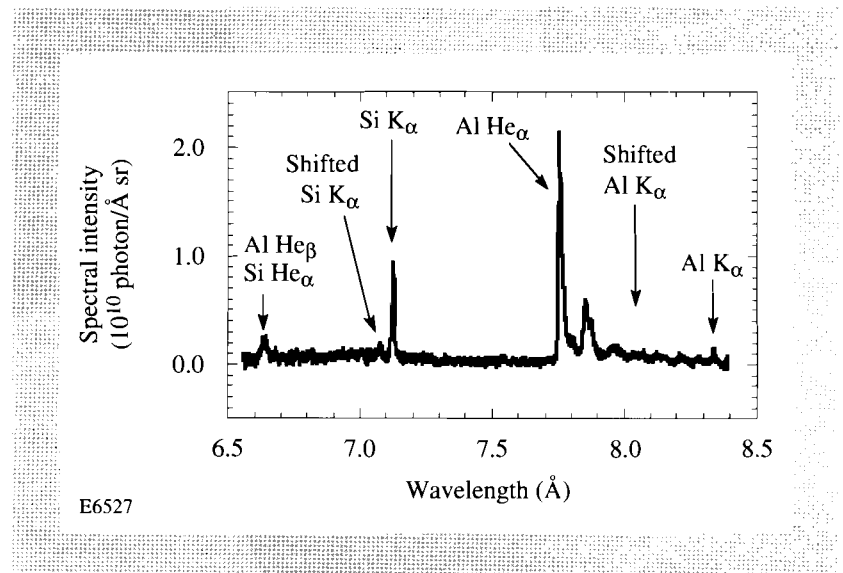


Fig. 54.13

Spectrum from an Si target coated with $0.2 \mu\text{m}$ Al, taken with a high-intensity-contrast laser pulse.

The K_{α} emission accounts for 55% of the emission into the spectral range from 6.5 Å to 8.5 Å. The total x-ray conversion efficiency into this range is $2 \times 10^{-3}\%/sr$. The Si K_{α} emission contributes $3 \times 10^{-4}\%/sr$. The conversion efficiency for the Al He_{α} line of $8 \times 10^{-4}\%/sr$ is somewhat lower than the value of $8 \times 10^{-3}\%/sr$ recently measured for a laser system with an ASE intensity below 10^{10} W/cm^2 .⁵ We believe that this may be caused by the shorter wavelength (0.248 μm) of this laser system, i.e., higher critical density, which may enhance collisional absorption of laser light, and a higher irradiance (10^{17} W/cm^2), which may result in a higher temperature and thus a higher fraction of He-like Al ions in the plasma.

The PIN diode filtered with 6 μm Al is mostly sensitive to Al K_{α} emission and 2.5-keV to 15-keV continuum emission since the Al He_{α} line and the Si K_{α} emission are strongly absorbed in the filter. Figure 54.14 shows the signal of this diode as a function of angle of incidence and polarization of laser light for a laser energy of 13 mJ and an Si target coated with 2.5 μm Al. The contribution of the 2.5-keV to 15-keV continuum emission to the detected x-ray signal was measured with a PIN diode filtered with 250 μm Be and was found to be 30%. Most of the x-ray signal is therefore caused by Al K_{α} emission; in Fig. 54.14 one unit of the y axis corresponds approximately to $3 \times 10^6 \text{ keV/sr}$ of Al K_{α} emission.

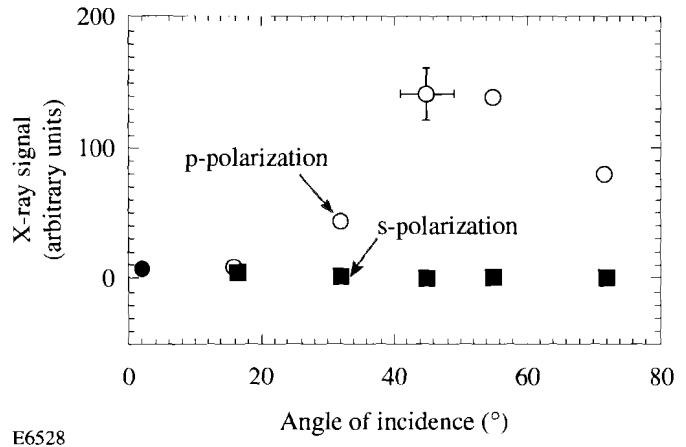


Fig. 54.14

Signal of a PIN diode filtered with 6 μm Al as a function of angle of incidence and polarization for high-intensity-contrast, 13-mJ laser pulses and an Si target coated with 2.5 μm Al. One unit on the y axis corresponds approximately to $3 \times 10^6 \text{ keV/sr}$ of Al K_{α} radiation.

The x-ray emission is seen to be maximum for p-polarized light at angle of incidence of around 50°. For s-polarized light, maximum x-ray emission is observed at perpendicular incidence. Nevertheless, the yield for s-polarization is more than one order of magnitude lower than the maximum yield observed for p-polarization. The strong polarization dependence at 50° is consistent with absorption measurements, which showed that 50% of p-polarized and 20% of s-polarized light are absorbed, respectively.⁷

The spectrum and the PIN diode filtered with 25 μm Be indicate that approximately 10^9 keV/sr of x rays with photon energies above the binding energy of an Si K-shell electron are emitted. From this we estimate that the

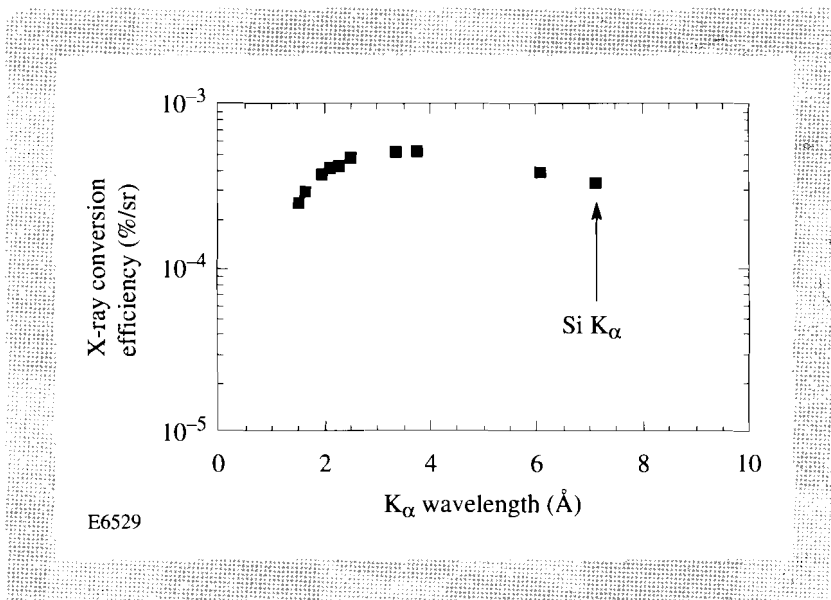
radiation-induced Si K_{α} yield is at most 10% of the measured value. Therefore, hot electrons appear to be the dominant source for the K_{α} emission. A Monte Carlo code was adapted to predict the K_{α} yield per electron as a function of angular distribution and energy distribution of the hot electrons, the thickness of the Al layer, and the Z number of the substrate material.¹⁹ In the simulations, backscattered electrons were recycled, i.e., they were made to reenter the target from the front, consistent with the reflection of hot electrons in the plasma sheath. It was further assumed that the target was a neutral solid. This limits, to some extent, the applicability of the predictions to measured data since the shifted K_{α} emission indicates (especially in the case of Al) that the material is partially ionized (Fig. 54.13). The hot-electron distribution may be characterized by comparing the code predictions to the observed dependence of the Si K_{α} yield on the thickness of the Al layer. In a previous experiment we found that a beamlike monoenergetic electron source as well as a plane-isotropic electron source with a Maxwellian energy distribution results in a good fit to the experimental data.¹⁰ Nevertheless, in the following analysis we will mostly concentrate on a Maxwellian energy distribution. This is reasonable since our measurements of the fast-ion blowoff of the plasma indicated Maxwellian-distributed electrons with a temperature scaling like $k_B T_h \sim 1.77 \times 10^{-5} I^{0.35}$ with $k_B T_h$ in keV and the irradiance I in W/cm^2 .⁸ A similar scaling law is predicted in particle-in-cell (PIC) simulations for resonantly heated electrons and $L/\lambda \sim 0.1$, where L is the density scale length and λ is the laser wavelength.²⁰ A process like resonance absorption may also explain the strong dependence of the Al K_{α} emission on angle of incidence and polarization of laser light observed in our experiment (Fig. 54.14). Recently, a similar dependence of the x-ray yield, integrated over a much wider spectral range, has been observed and attributed to a process with the characteristics of resonance absorption.²

For an estimate of the hot-electron temperature $k_B T_h$ we will use the scaling law obtained from our fast-ion measurements⁸ and PIC simulations²⁰ rather than the value recently measured from the slope of the Si K_{α} yield versus Al thickness¹⁰ since the latter experiment was done with slightly different experimental parameters. For an irradiance of $4 \times 10^{15} \text{ W}/\text{cm}^2$ we calculate $k_B T_h \sim 5 \text{ keV}$. By matching the predicted Si K_{α} yield per electron to the measured yield, we estimate that for electrons with a temperature of 5 keV, 25% of the laser energy is deposited into the target. For 10-keV electrons 15% is calculated. On the other hand, measurements of the ion blowoff also showed that less than 5% of the laser energy appeared in the fast ions. This indicates that most of the hot-electron energy is deposited into the target.

For substrates with a higher Z number the K_{α} emission shifts toward shorter wavelength. Figure 54.15 shows the x-ray conversion efficiency predicted by Monte Carlo simulations for various Z -substrates coated with $0.2 \mu\text{m}$ Al as a function of K_{α} wavelength. In the simulation, 5-keV electrons carrying 25% of the laser energy were assumed for all target configurations since the characteristics of the hot electrons are predominantly determined by the interaction of the laser pulse with the Al layer. It can be seen that at 1.5 \AA , i.e., for Cu K_{α} emission, the x-ray conversion efficiency is still above $2 \times 10^{-4} \text{ %/sr}$ and thus comparable to the value for the Si K_{α} emission.

Fig. 54.15

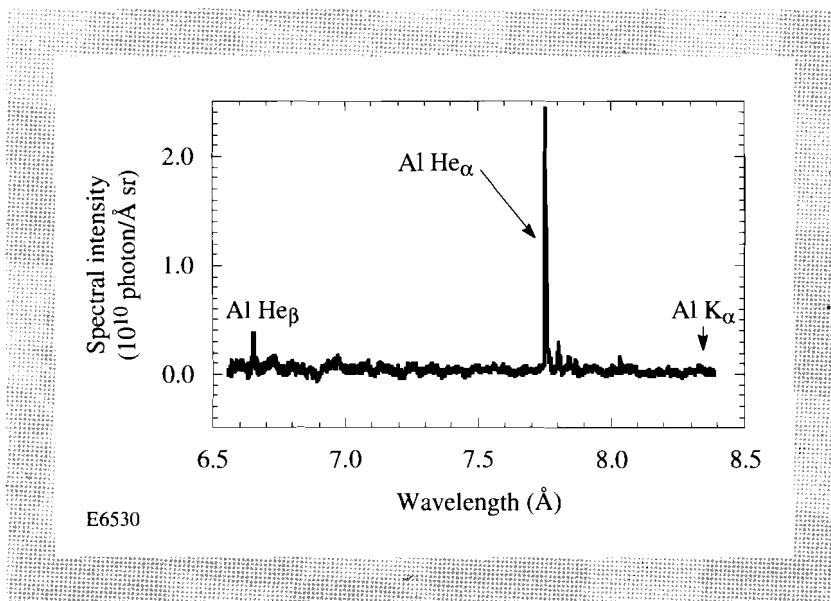
Predicted x-ray conversion efficiency into K_{α} emission as a function of K_{α} wavelength. The substrate materials are coated with $0.2 \mu\text{m}$ Al. 25% of the laser energy is absorbed by hot electrons with a temperature of 5 keV.



The spectrum taken for a low-intensity-contrast laser pulse, i.e., a prepulse irradiance of $\sim 4 \times 10^{12} \text{ W/cm}^2$, shows mostly Al He_{α} emission but hardly any Al and Si K_{α} emission (Fig. 54.16). The He_{α} line is approximately 10% higher than in the case of a high-intensity-contrast laser pulse (Fig. 54.13), but the total x-ray emission into the spectral range of 6.5 \AA to 8.5 \AA is 60% lower. Since a low-intensity contrast will result in a preformed plasma, the scale length of the plasma interacting with the main pulse is longer than for a high-intensity-contrast laser pulse. In long-scale-length plasma resonance absorption is expected to be less efficient at the relatively large angle of incidence chosen in this experiment.²¹ In addition, other absorption mechanisms, like inverse bremsstrahlung absorption that does not generate significant numbers of hot electrons, may be dominant. Therefore the K_{α} production shows a strong dependence on the level of prepulse.

Fig. 54.16

Spectrum from an Si target coated with $0.2 \mu\text{m}$ Al, taken with a low-intensity-contrast laser pulse.



2. Temporal Evolution of X-Ray Emission and X-Ray Source Size

The streak-camera recordings of the x-ray emission from an SiO_2 target coated with $0.6 \mu\text{m Al}$ are shown in Fig. 54.17 for a high-intensity-contrast laser pulse. From the PIN-diode measurements and the spectral sensitivity of CsI^{22} we estimate that $\sim 80\%$ of the signal of the Al channel is caused by Al K_α emission, and $\sim 50\%$ of the signal of the Be channel is caused by Al He_α emission. The streak-camera measurements indicate a duration of 10 ps (FWHM) for the Be channel and 8 ps for the Al channel. The actual duration of emission may well be shorter than 10 ps and 8 ps, respectively, since a temporal resolution of the streak camera of around 7 ps will broaden the detected signal. The Mylar channel indicates that the soft x-ray emission lasted around 20 ps. In the case of a low-intensity-contrast laser pulse both the Be channel and the Mylar channel show a longer duration of emission, i.e., 13 ps and 70 ps, respectively. The Al channel detected no signal, consistent with the low levels of Al K_α emission observed in the spectrum for a low-intensity-contrast laser pulse (Fig. 54.16).

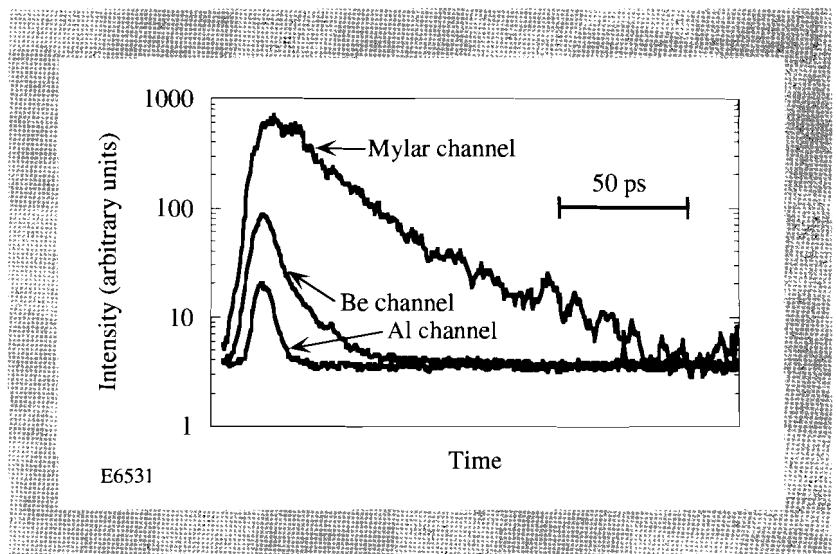


Fig. 54.17
Streak-camera trace from an SiO_2 target coated with $0.6 \mu\text{m Al}$, taken with a high-intensity-contrast laser pulse. The temporal evolution of the Mylar, Be, and Al channels is shown.

Even for a high-intensity contrast the duration of the He_α line is longer than the laser-pulse duration itself; it depends on recombination processes and the cooling of the plasma. On the other hand, the duration of the K_α emission is determined by time scales of processes, such as hot-electron production, energy deposition, and lifetime of excited ions. In the case of hot electrons generated by wavebreaking, an upper limit for the time elapsed between the end of the laser pulse and the end of hot-electron production may be estimated from the damping time of the plasma wave. For collisional damping, the damping rate roughly equals the electron-ion collision frequency,²³ which is around 10^{14} s^{-1} at critical density for a 300-eV temperature. Hot electrons are thus probably generated only during the interaction of the laser pulse with the plasma. For hot electrons penetrating the target, the time scale of the energy deposition may be estimated in the nonrelativistic case from the stopping time in the target.²⁴ Electrons with a temperature of 5 keV are predicted to have an average stopping time of 0.2 ps.

The excited states involved in the K_α emission process have a short lifetime (femtosecond range).²⁵ Therefore, the duration of the K_α emission is probably

dominated by the time scale of the hot-electron generation and should be below a few picoseconds, consistent with the duration of the measured signal in the Al channel. Nevertheless, the effect of self-generated magnetic fields, especially at higher irradiance, on the x-ray pulse duration may require further investigations to explain the duration of Al K_{α} emission recently observed in other experiments.²⁶

The x-ray shadowgraph indicated that the plasma region emitting x rays above ~ 1 keV is approximately equal to the focal spot of the laser. No direct evidence for substantial K_{α} emission from a much larger area, as would be expected for lateral transport, could be found.

Conclusions

We have observed strong K_{α} emission in high-intensity-contrast, picosecond, p-polarized laser-plasma interactions. The K_{α} emission was found to be induced by hot electrons. The strong dependence of the K_{α} emission on angle of incidence and polarization of laser light is consistent with hot electrons generated by resonance absorption. With a duration of emission of ≤ 8 ps, a source area of $1.6 \times 10^{-6} \text{ cm}^2$, and an x-ray yield at 7.1 \AA of 1.5×10^8 photon/sr, a radiance of $\geq 3 \times 10^9 \text{ W/cm}^2 \text{ sr}$ is calculated. This value is three orders of magnitude lower than the radiance of the Al L_{α} line recently reported for a $0.3\text{-}\mu\text{m}$, 290-fs laser system at a much higher irradiance of $5 \times 10^{18} \text{ W/cm}^2$.²⁷ Nevertheless, K_{α} emission has the potential to generate shorter x-ray pulses than, for example, resonance line emission because its duration of emission depends on processes such as hot-electron production and energy deposition rather than on recombination and cooling processes in the plasma.

The K_{α} emission is a promising candidate to obtain an efficient, ultrashort x-ray source at short wavelength. The analysis suggested that, for example, Cu K_{α} emission ($\lambda \sim 1.5 \text{ \AA}$) may be obtained at an irradiance of $4 \times 10^{15} \text{ W/cm}^2$. By choosing the appropriate fluor material and laser intensity, the x-ray conversion efficiency as well as the K_{α} wavelength may be further optimized.

ACKNOWLEDGMENT

This work is supported by the U.S. Department of Energy Office of Inertial Confinement Fusion under Cooperative Agreement No. DE-FC03-92SF19460 and the University of Rochester and by the Swiss National Science Foundation. The support of the DOE does not constitute an endorsement by DOE of the views expressed in this article.

REFERENCES

1. M. M. Murnane, H. C. Kapteyn, and R. W. Falcone, *IEEE J. Quantum Electron.* **25**, 2417 (1989).
2. U. Teubner *et al.*, *Phys. Rev. Lett.* **70**, 794 (1993).
3. H. W. K. Tom and O. R. Wood II, *Appl. Phys. Lett.* **54**, 517 (1989).
4. U. Teubner, G. Kühnle, and F. P. Schäfer, *Appl. Phys. Lett.* **59**, 2672 (1991).
5. J. A. Cobble *et al.*, *J. Appl. Phys.* **69**, 3369 (1991).
6. J. C. Kieffer, *Bull. Am. Phys. Soc.* **37**, 1468 (1992).
7. S. Uchida, H. Chen, Y.-H. Chuang, J. A. Delettrez, and D. D. Meyerhofer, *Bull. Am. Phys. Soc.* **36**, 2304 (1991).

8. D. D. Meyerhofer, H. Chen, J. Delettrez, B. Soom, S. Uchida, and B. Yaakobi, to be published in *Physics of Fluids B*.
9. P. Audebert *et al.*, *Europhys. Lett.* **19**, 189 (1992).
10. H. Chen, B. Soom, B. Yaakobi, and D. D. Meyerhofer, submitted to *Physical Review Letters*.
11. P. Maine, D. Strickland, P. Bado, M. Pessot, and G. Mourou, *IEEE J. Quantum Electron.* **24**, 398 (1988).
12. Y.-H. Chuang, D. D. Meyerhofer, S. Augst, H. Chen, J. Peatross, and S. Uchida, *J. Opt. Soc. Am. B* **8**, 1226 (1991).
13. B. Yaakobi, R. E. Turner, H. W. Schnopper, and P. O. Taylor, *Rev. Sci. Instrum.* **50**, 1609 (1979).
14. R. Hall *et al.*, *X-Ray Spectrom.* **8**, 20 (1979).
15. B. L. Henke *et al.*, *J. Opt. Soc. Am. B* **3**, 1540 (1986).
16. M. M. Murnane, H. C. Kapteyn, and R. W. Falcone, *Appl. Phys. Lett.* **56**, 1948 (1990).
17. B. L. Henke, J. Liesegang, and S. D. Smith, *Phys. Rev. B* **19**, 3004 (1979).
18. Ph. Alaterre *et al.*, *Opt. Commun.* **49**, 140 (1984).
19. B. Luther-Davies, A. Perry, and K. A. Nugent, *Phys. Rev. A* **35**, 4306 (1987).
20. P. Gibbon and A. R. Bell, *Phys. Rev. Lett.* **68**, 1535 (1992).
21. K. G. Estabrook, E. J. Valeo, and W. L. Kruer, *Phys. Fluids* **18**, 1151 (1975).
22. B. L. Henke, J. P. Knauer, and K. Premaratne, *J. Appl. Phys.* **52**, 1509 (1981).
23. W. L. Kruer, *The Physics of Laser Plasma Interactions* (Addison-Wesley, Redwood City, CA, 1988), Vol. 73.
24. B. Soom, H. Chen, and D. D. Meyerhofer, in *Short-Pulse High-Intensity Lasers and Applications II* (SPIE, Bellingham, WA, 1993), Vol. 1860, to be published.
25. T. W. Tunnell, C. Can, and C. P. Bhalla, *J. Quant. Spectrosc. Radiat. Transfer* **27**, 405 (1982).
26. J. C. Kieffer, in *Short-Pulse High-Intensity Lasers and Applications II* (SPIE, Bellingham, WA, 1993), Vol. 1860, to be published.
27. G. A. Kyrala *et al.*, *Appl. Phys. Lett.* **60**, 2195 (1992).